

Tracking the dynamics of pathogen interactions: Modeling ecological and immune-mediated processes in a two-pathogen single-host system

Daniel A. Vasco^{a,*}, Helen J. Wearing^a, Pejman Rohani^{a,b}

^a*Institute of Ecology, University of Georgia, Athens, GA 30602, USA*

^b*Center for Tropical and Emerging Global Diseases, University of Georgia, Athens, GA 30602, USA*

Received 16 November 2005; received in revised form 17 July 2006; accepted 21 August 2006

Available online 30 August 2006

Abstract

Traditionally, epidemiological studies have focused on understanding the dynamics of a single pathogen, assuming no interactions with other pathogens. Recently, a large body of work has begun to explore the effects of immune-mediated interactions, arising from cross-immunity and antibody-dependent enhancement, between related pathogen strains. In addition, ecological processes such as a temporary period of convalescence and pathogen-induced mortality have led to the concept of ecological interference between unrelated diseases. There remains, however, the need for a systematic study of both immunological and ecological processes within a single framework. In this paper, we develop a general two-pathogen single-host model of pathogen interactions that simultaneously incorporates these mechanisms. We are then able to mechanistically explore how immunoeological processes mediate interactions between diseases for a pool of susceptible individuals. We show that the precise nature of the interaction can induce either competitive or cooperative associations between pathogens. Understanding the dynamic implications of multi-pathogen associations has potentially important public health consequences. Such a framework may be especially helpful in disentangling the effects of partially cross-immunizing infections that affect populations with a pre-disposition towards immunosuppression such as children and the elderly.

© 2006 Elsevier Ltd. All rights reserved.

Keywords: Infectious disease modeling; Ecological interference; Immune-mediated processes

1. Introduction

Outbreaks of diseases such as SARS, West Nile Virus and avian influenza have alerted us to the potentially grave public health threat from emerging and re-emerging pathogens (Cyranoski, 2001; Lipsitch et al., 2003; Mackenzie et al., 2004). However, understanding the persistence, spread and evolution of extant pathogens also remains a significant challenge. Historically, our understanding of disease-host systems has been built upon a population-based rather than community-based approach: epidemiologists have traditionally studied infectious disease at the level of a single pathogen species infecting a single-host species. This has led to a significant body of epidemiological research devoted to understanding the precise mechanisms underlying host–pathogen dynamics in isola-

tion. In the case of novel emerging pathogens, this is perhaps a reasonable study unit. In the case of established pathogens, however, it may well be an oversimplification of the web of ecological and immunological interactions in which hosts and their pathogens persist and evolve.

During the past several years, single-host single-pathogen approaches have been extended to incorporate multiple hosts (Hudson and Greenman, 1998; Gog et al., 2002; Dobson, 2004) and multiple pathogens (Gupta et al., 1994; Ferguson et al., 2003). Much of the work on multi-host systems has focused on how parasites can shape host coexistence dynamics by mediating “apparent” competition between host species (Holt, 1977; Tomkins et al., 2001). However, the area of community epidemiology that has received most attention has been the dynamics of multi-strain pathogens, in part due to the number and importance of microparasites with well-established antigenic polymorphism, such as influenza, malaria, the adenoviruses, poliovirus and cholera (Andreasen et al.,

*Corresponding author. Tel.: +1 7065423580.
E-mail address: vasco@uga.edu (D.A. Vasco).

1997; Gupta et al., 1998; Read and Taylor, 2001; Earn et al., 2002; Koelle et al., 2005). In such systems, it is empirically documented that different strains typically fluctuate out-of-phase with each other; epidemics of one strain do not generally coincide with epidemics of another. Multi-strain interactions have been studied on two distinct scales: within-host immune-mediated interactions such as superinfection and coinfection (Nowak and May, 1994; Kirschner, 1999); and between-host immune-mediated interactions such as cross-immunity and antibody-dependent enhancement (Ferguson et al., 1999; Cummings et al., 2005). In particular, the significance of partial cross-immunity in shaping the coexistence, dynamics and evolution of strains has been at the core of a large body of work (Elveback et al., 1968; Dietz, 1979; White et al., 1998; Gog et al., 2002; Kamo and Sasaki, 2002; Abu-Raddad and Ferguson, 2004; Pease, 1987).

Until recently, however, the possibility that epidemics of *unrelated* pathogens might interact has been ignored. Rohani et al. (1998) proposed an ecological mechanism—termed interference—that may contribute to interaction among unrelated acute infections. This ecological interference arises from the (temporary or permanent) removal of potential hosts from the susceptible population for one infection following an infection by one of its direct competitors. The primary mechanism for removal is the convalescent period, during which individuals are in quarantine and hence unavailable to contract “competing” infections. In addition, depending upon the disease and host age and condition, individuals may suffer death as a result of infection, in which case removal from the susceptible pool becomes permanent and the competitive interaction between pathogens is predicted to become stronger. Ecological interference has similar dynamical consequences to cross-immunity in strain polymorphic systems, whereby individuals previously infected with one strain may have partial protection to other competing strains (Kamo and Sasaki, 2002). The significant prediction of the Rohani et al. (1998) model was that epidemics of competing infections would be temporally segregated, with major outbreaks out-of-phase with each other (Huang and Rohani, 2005, 2006; Rohani et al., 2006). Empirical support for interference effects is provided in case fatality data for measles and whooping cough for several European cities in the pre- and post-WWI eras when birth rates were high and infection was associated with significant mortality (Rohani et al., 2003), conditions which remain pervasive in many developing countries today.

In addition to ecological interactions, unrelated pathogens may also interact through immune-mediated responses. This is likely to take place via a host’s innate, non-specific immune response rather than the acquired, specific response that mediates interactions such as cross-immunity and antibody-dependent enhancement between similar pathogen strains. There are perhaps two main ways for this interaction to occur. First, during the initial stages of infection, the host’s innate immune response is strongly

activated and may temporarily prevent the establishment of other infections. Second, following infection with certain pathogens (e.g. measles and influenza), a host’s immune system is suppressed for a period of time during which an individual may be more prone to colonization by other (particularly bacterial) infections (Openshaw and Tregoning, 2005; Openshaw, 2005; Thompson et al., 2003). In this case, prior infection with one pathogen may actually facilitate infection by another, unrelated pathogen. When infection occurs by certain enteroviruses, it is thought that tissue damage triggers a severe immunosuppressive response within patients and that this “primes” the patient for other pathogens by inducing dilated cardiomyopathy and chronic inflammatory myopathy (Klingel et al., 1992). Another well-studied example is infection with human immunodeficiency virus (HIV) which has been shown to increase susceptibility to infection with many other pathogens and parasites (Corbett et al., 2002), and, in particular, with *Mycobacterium tuberculosis* (TB) (Porco et al., 2001; Corbett et al., 2003). Dynamically, these kinds of mechanisms leading to immunosuppression between unrelated pathogens should exhibit strong similarities with antibody-dependent enhancement between antigenically-related pathogens, whereby individuals previously infected with one strain may experience more severe disease when infected with a second strain (e.g. dengue serotypes (Halstead, 1970)). So far, however, a dynamical exploration of immunosuppression as a mode of interaction between pathogens has been lacking.

This body of past work makes clear that related and unrelated pathogens can potentially interact through a variety of immunological and ecological mechanisms, many of which share common dynamical outcomes. However, a systematic study of the different possible routes of interaction between different infections is still lacking. In this paper, we aim to fill this gap by developing a general model for examining systems with multiple pathogens. The proposed framework is flexible and may be applied to strain polymorphic as well as to unrelated diseases. The key ingredient of the formalism we develop is the simultaneous inclusion of immune-mediated components (coinfection, immunosuppression/cross-enhancement and cross-immunity) and ecological factors (quarantine and infection-induced mortality). Our approach is to generalize the transmission process within a two-pathogen single-host community. An important feature is that the framework is built around a null model of no interaction, which allows us to demonstrate how pathogen interaction changes single-pathogen single-host dynamics in a predictable manner. We then use this framework to track the dynamics of pathogen interactions over the immunoeological “landscape”. Specifically, we focus on four static and dynamical properties of the two-pathogen system: coexistence and stability of equilibria, and period and phase of periodic attractors. We demonstrate how a suite of immunoeological interactions between pathogens in a two-disease community can lead to transient or sustained

oscillations in disease prevalence. These fluctuations may be either asynchronous if competition is strong or synchronous if cooperation is induced. Furthermore, we show how the period of the two-disease attractor is affected by key immunoeological interactions. The theory we use is based upon numerical explorations of two key eigenmodes (eigenvalue–eigenvector pairs). Although this paper does not directly address the influence of seasonality, these signatures are crucial for gaining insight into the system trajectories observed under periodic forcing, and the patterns we might expect to observe in epidemiological data.

2. A generalized two-pathogen single-host model

Our generalized model builds on the traditional concept of the *SEIR* (susceptible, exposed, infected, recovered) paradigm (Kermack and McKendrick, 1927; Anderson and May, 1991). In this framework an individual is categorized according to their infection status and passes sequentially through the series of *SEIR* classes. As mentioned in the Introduction, various models have been developed in an attempt to generalize this approach to include interactions between different pathogens. In this paper we combine several of these approaches into a single model. Specifically, ecological interactions between pathogens, such as a period of convalescence (Rohani et al., 1998, 2003) or disease-induced mortality (Huang and Rohani, 2005) are incorporated as well as immune-mediated interactions such as coinfection (Nowak and May, 1995), cross-immunity (Kamo and Sasaki, 2002), or cross-enhancement (Ferguson et al., 1999) and immunosuppression. This allows a systematic investigation of these dynamical processes within a unified modeling framework. We incorporate the basic elements required to describe the natural history of two distinct infections of a single host:

1. All new-borns are fully susceptible to both infections.
2. Upon infection, a susceptible individual enters the exposed (infected but not yet infectious) class, and has a relative probability of contracting the other disease simultaneously, modulated by the coinfection parameter, ϕ_i ($i = 1, 2$).
3. After a latent period, the individual becomes infectious and still has the same chance of contracting the other disease (ϕ_i , $i = 1, 2$). We note that coinfection is not a competitive process within the host in the current model: if coinfection occurs both infections are allowed to run their course.
4. Often when symptoms appear, the disease is diagnosed and the individual enters a convalescent phase for an average period given by $1/\delta_i$ ($i = 1, 2$). During convalescence, the other infection may be contracted but the transmission rate is modulated by the parameter ξ_i ($i = 1, 2$). If $0 \leq \xi_i < 1$, convalescence may represent a period of quarantine (reduced contact rates) or temporary cross-immunity (reduced susceptibility). If $\xi_i > 1$,

convalescence may represent, via increased susceptibility, immunosuppression (non-related pathogens) or cross-enhancement (antigenically related pathogens).

5. Depending upon the pathogen and host age and condition, an infection may be fatal, often due to complications (such as pneumonia and encephalitis, in the case of measles and pertussis). This is represented by per capita infection-induced mortality probabilities ρ_i ($i = 1, 2$).
6. Upon complete recovery, the individual is assumed immune to the first infection but remains susceptible to the second infection, if not previously exposed to it. At this stage, we introduce the term χ_i to explore the implications of long-lasting cross-immunity ($\chi_i < 1$) or cross-enhancement/immunosuppression ($\chi_i > 1$) for the transmission rate of disease i following infection with disease j .
7. An alternative way of introducing cross-immunity and cross-enhancement is by assuming that infectiousness, rather than susceptibility, is altered. We incorporate this using the parameter η_i , so that comparisons can be made with previous models that have used this representation. If $\eta_i < 1$ then those contracting infection i after the other infection will be less infectious (or equivalently only a proportion η_i will transmit the infection), if $\eta_i > 1$ they will be more infectious.

We note that for parameters describing the interaction between pathogens (ϕ_i , χ_i , ξ_i , η_i , $i = 1, 2$) the subscript always refers to the infecting pathogen.

The mathematical representation of these assumptions is presented as the following system of ordinary differential equations:

$$\frac{dS_0}{dt} = \nu N - (\lambda_1 + \lambda_2) \frac{S_0}{N} - \mu S_0,$$

$$\frac{dE_1}{dt} = \lambda_1 \frac{S_0}{N} - \phi_2 \lambda_2 \frac{E_1}{N} - (\sigma_1 + \mu) E_1,$$

$$\frac{dI_1}{dt} = \sigma_1 E_1 - \phi_2 \lambda_2 \frac{I_1}{N} - (\gamma_1 + \mu) I_1,$$

$$\frac{dC_1}{dt} = \gamma_1 I_1 - \xi_2 \lambda_2 \frac{C_1}{N} - (\delta_1 + \mu) C_1,$$

$$\frac{dS_1}{dt} = (1 - \rho_1) \delta_1 C_1 - \chi_2 \lambda_2 \frac{S_1}{N} - \mu S_1,$$

$$\frac{dE_2}{dt} = \lambda_2 \frac{S_0}{N} - \phi_1 \lambda_1 \frac{E_2}{N} - (\sigma_2 + \mu) E_2,$$

$$\frac{dI_2}{dt} = \sigma_2 E_2 - \phi_1 \lambda_1 \frac{I_2}{N} - (\gamma_2 + \mu) I_2,$$

$$\frac{dC_2}{dt} = \gamma_2 I_2 - \xi_1 \lambda_1 \frac{C_2}{N} - (\delta_2 + \mu) C_2,$$

$$\frac{dS_2}{dt} = (1 - \rho_2) \delta_2 C_2 - \chi_1 \lambda_1 \frac{S_2}{N} - \mu S_2,$$

$$\begin{aligned}
\frac{dS_{12}}{dt} &= (1 - \rho_1)(1 - \rho_2) \left(\phi_2 \lambda_2 \frac{E_1 + I_1}{N} + \xi_2 \lambda_2 \frac{C_1}{N} \right. \\
&\quad \left. + \phi_1 \lambda_1 \frac{E_2 + I_2}{N} + \xi_1 \lambda_1 \frac{C_2}{N} \right) \\
&\quad + (1 - \rho_2) \chi_2 \lambda_2 \frac{S_1}{N} + (1 - \rho_1) \chi_1 \lambda_1 \frac{S_2}{N} - \mu S_{12}, \\
\frac{d\varepsilon_1}{dt} &= \lambda_1 \frac{S_0}{N} + \eta_1 \left(\phi_1 \lambda_1 \frac{E_2 + I_2}{N} + \xi_1 \lambda_1 \frac{C_2}{N} + \chi_1 \lambda_1 \frac{S_2}{N} \right) \\
&\quad - (\sigma_1 + \mu) \varepsilon_1, \\
\frac{d\varepsilon_2}{dt} &= \lambda_2 \frac{S_0}{N} + \eta_2 \left(\phi_2 \lambda_2 \frac{E_1 + I_1}{N} + \xi_2 \lambda_2 \frac{C_1}{N} + \chi_2 \lambda_2 \frac{S_1}{N} \right) \\
&\quad - (\sigma_2 + \mu) \varepsilon_2, \\
\frac{d\lambda_1}{dt} &= \beta_1 \sigma_1 \varepsilon_1 - (\gamma_1 + \mu) \lambda_1, \\
\frac{d\lambda_2}{dt} &= \beta_2 \sigma_2 \varepsilon_2 - (\gamma_2 + \mu) \lambda_2, \tag{1}
\end{aligned}$$

where the class of all those susceptible to both infections is denoted by S_0 . The variables E_i , I_i and C_i ($i = 1, 2$) represent those currently exposed, infectious or convalescing (respectively) after infection with disease i , with no previous exposure to any infection. The terms S_i ($i = 1, 2$) represent all individuals that are recovered from infection i but still susceptible to infection j . For bookkeeping purposes we let ε_i and λ_i represent the forces of latency and infection for pathogen i ($i = 1, 2$). Additionally, note that S_{12} are all those no longer susceptible to either infection, and may include those who are still exposed or infectious with one or both diseases (i.e. included within ε_1 , ε_2 , λ_1 or λ_2). The model parameters are explained in Table 1.

In this paper, N represents the total population size in the absence of disease-induced mortality, which is defined to be constant by setting $v = \mu$. In the presence of disease-induced mortality, we do not reduce N when calculating

frequency-dependent transmission since we want to ensure that the level of mixing/contact remains the same. With this assumption, the S_{12} class plays no dynamic role in the system (see Appendix A for further details on how this system of equations is derived from first principles). It is also worth noting that historically, disease-induced mortality has been incorporated into epidemiological models by the addition of a mortality term to equations describing the dynamics of infected. While this formulation may be appropriate for some pathogens, a re-think is needed when considering diseases such as measles and whooping cough. Here, individuals may succumb to the pathogen as a result of complications from the infection, such as hypoxia, encephalitis or secondary lung infections, which typically occur long after the effective infectious period has elapsed (Behrman and Kliegman, 1998). Hence, we have chosen to model this as the probability a convalescing individual successfully re-enters the population.

We point out that most previous models investigating the interactions of two pathogens and a single host are nested within this generalized model as limiting cases of certain parameters. In particular, setting $\phi_i = \xi_i = 0$, $\chi_i = \eta_i = 1$ for $i = 1, 2$ we arrive at the extension by Huang and Rohani (2005) to the ecological interference model of Rohani et al. (1998). Furthermore, the lower dimensional models analysed by Ferguson et al. (1999) (which is a two-strain version of a model formulated in Gupta et al. (1998) and Kamo and Sasaki (2002)) can be derived if $1/\sigma_i \rightarrow 0$ and $\phi_i = \xi_i = \chi_i = 1$, and $1/\sigma_i \rightarrow 0$ and $\phi_i = \xi_i = \chi_i, \eta_i = 1$, respectively.

3. Equilibria, invasability and coexistence

We now investigate the equilibrium properties of our two-disease model with respect to changes in model parameters. When the disease transmission coefficients (β_i) are constants, as we assume throughout this paper, it can be shown that there are four possible equilibria: (i) the disease-free equilibrium; (ii) two single disease equilibria

Table 1
Description of model parameters

Parameter	Epidemiological description	Typical range
v	Per capita birth rate	1/40–1/75 yr ⁻¹
μ	Per capita death rate	1/40–1/75 yr ⁻¹
$1/\sigma_i$	Average latent period	1–15 days
$1/\gamma_i$	Average infectious period	1–20 days
$1/\delta_i$	Average convalescent period	0–9 months
ρ_i	Probability of infection-induced mortality	0–1
ϕ_i	Relative probability of coinfection with infection i	0–1
ξ_i	Temporary quarantine/cross-immunity to infection i	0–1
ζ_i	Temporary immunosuppression/cross-enhancement to infection i	> 1
χ_i	Permanent cross-immunity to infection i	0–1
λ_i	Permanent immunosuppression/cross-enhancement to infection i	> 1
η_i	Alternative permanent cross-immunity to infection i	0–1
η_i	Alternative permanent cross-enhancement to infection i	> 1
β_i	Transmission rate	100–2000 yr ⁻¹

and (iii) the two-disease coexistence equilibrium. Conditions for demonstrating the existence and computation of these equilibria are developed in the Appendix. We show that equilibrium values for all state variables of this dynamical system are uniquely determined by numerically solving two coupled equations in terms of the forces of infection (λ_1, λ_2).

Given the number of parameters in our model, one might expect a range of different effects on these equilibria. Intuitively, one possible consequence of pathogen interactions among infections is reduced abundance. Surprisingly, however, detailed analyses have demonstrated that ecological interference does not manifest itself by significantly altering infection prevalence; changes in model parameters such as the convalescent period translate into negligible changes in the number of infectives of either infection (Huang and Rohani, 2005). Perhaps more surprisingly, ecological factors have been shown to exert little influence on the coexistence likelihood of pathogens. To demonstrate in detail how the different immunological and ecological parameters of the generalized model affect the possibility of pathogen coexistence, we now state the invasibility criterion. Given that the basic reproductive ratio of each disease is determined by

$$R_0^i = \frac{\beta_i \sigma_i}{(\sigma_i + \mu)(\gamma_i + \mu)}, \quad i = 1, 2,$$

it is then straightforward to show that pathogen j can only invade the single-disease equilibrium of pathogen i if

$$R_0^j > \frac{R_0^i}{1 + a_i(R_0^i - 1)} \quad \text{where } R_0^i > 1 \quad (2)$$

and

$$a_i = \frac{\eta_j}{\sigma_i + \mu} \left(\phi_j \mu + \frac{\sigma_i}{\gamma_i + \mu} \left(\phi_j \mu + \frac{\gamma_i}{\delta_i + \mu} (\xi_j \mu + \chi_j (1 - \rho_i) \delta_i) \right) \right), \quad (3)$$

for $i, j = 1, 2$ and $i \neq j$. Of greater insight is that $a_i \approx \eta_j \chi_j (1 - \rho_i)$ under a fairly non-restrictive set of assumptions: namely, that host lifespan is significantly greater than the length of the latent, infectious and convalescent periods ($\mu \ll \sigma_i, \gamma_i, \delta_i$) and that ξ_j and η_j are not too large ($\eta_j \phi_j \mu \ll \sigma_i, \gamma_i$ and $\eta_j \xi_j \mu \ll \delta_i$). For a limiting case of this model ($\phi_i = \xi_i = 0, \chi_i = \eta_i = 1, i, j = 1, 2$), Gumel et al. (2003) showed that the two disease coexistence equilibrium must be stable when both single-disease equilibria lose their stability, and this appears to hold for the general model presented here. Fig. 1 illustrates how condition (2) affects the coexistence of the two diseases as a function of the key parameters ρ ($= \rho_1 = \rho_2$ assuming symmetry) and χ ($= \chi_1 = \chi_2$ assuming symmetry, which is equivalent to varying $\eta = \eta_1 = \eta_2$). Disease-induced mortality ($\rho > 0$) decreases the region of coexistence in exactly the same way as permanent cross-immunity after infection ($\chi < 1$): at the population level, these two mechanisms have the same dynamical consequences. However, immune-mediated interactions may also act in the opposite direction: if

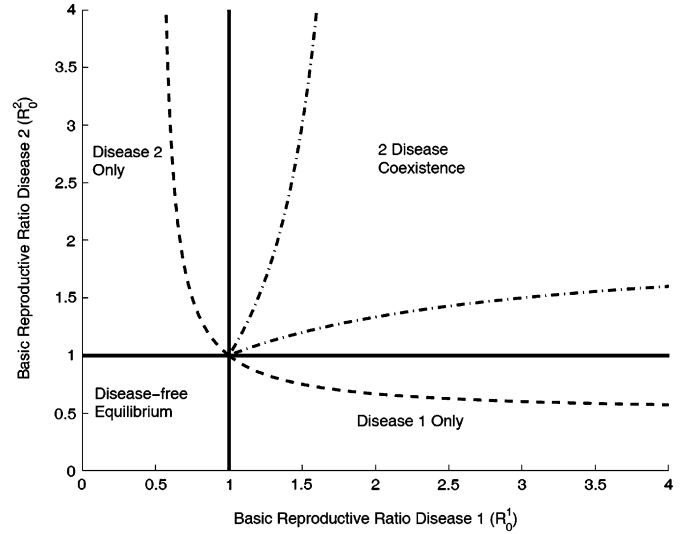


Fig. 1. Invasibility diagram determining two-pathogen coexistence. This figure demonstrates that coexistence of the two infections can be affected by immunosuppression and disease-induced mortality. In the absence of immune-mediated interactions ($\phi_i = \xi_i = \chi_i = 1, i = 1, 2$), large levels of disease-induced mortality (a 50% level is shown on the dot-dashed line), can cause the region of two-disease coexistence to shrink. In contrast, strong levels of permanent immunosuppression ($\phi_i = \xi_i = 1, \chi_i = 2, \rho_i = 0, i = 1, 2$) can expand the coexistence domain (dashed line). Epidemiological parameters used to construct this diagram were for measles (labeled disease 1 in figure) and pertussis (labeled disease 2 in figure) and are given in Table 2.

infection with one pathogen in some way primes the host for infection with another ($\chi > 1$), the coexistence region can significantly expand, so that one disease can invade another even if its R_0 is below 1.

4. Stability and qualitative dynamics of the model

In simple host–pathogen models, for $R_0 > 1$, the system exhibits damped oscillations towards a globally stable endemic equilibrium. However, when competitive or cooperative interactions between pathogens are permitted, ecological theory would suggest that a range of dynamical outcomes is possible. In this section our emphasis is on using linear stability analysis of the pathogen coexistence equilibrium, guided by numerical integration of the full nonlinear system, to describe pathogen dynamics for a number of different epidemiological scenarios. For each scenario, a two-parameter bifurcation diagram illustrates the stability of the coexistence equilibrium, and, when it is unstable, the qualitative oscillatory dynamics we expect to observe. These explorations of parameter space are divided into those that are possible for multi-strain (related) pathogens and those that are possible for unrelated pathogens. In addition, for the analyses of dynamics presented in this paper, we will focus on interactions involving host susceptibility rather than infectiousness and assume that $\eta_i = 1$ ($i = 1, 2$). For purposes of illustration, we adopt three baseline sets of parameter values from well-studied childhood diseases (Anderson and May, 1991)

Table 2
Baseline parameter sets used in the epidemic modeling

Parameter	Measles	Pertussis	Rubella
$1/\sigma$	8 days	8 days	9 days
$1/\gamma$	5 days	10 days	11 days
$1/\delta$	7 days	14 days	14 days
R_0	17	17	7
$\beta = \frac{R_0(\gamma + \mu)(\sigma + \mu)}{\sigma}$	1242 yr ⁻¹	621 yr ⁻¹	233 yr ⁻¹
$T_I \sim 2\pi \sqrt{\frac{1}{\mu(R_0 - 1)} \left(\frac{1}{\mu + \sigma} + \frac{1}{\mu + \gamma} \right)}$	2.1 yr	2.5 yr	4.2 yr

(see Table 2). However, in some analyses we also allow epidemiological parameters to vary in addition to those modulating pathogen interactions. In this section we do not systematically vary the birth rate (μ) or disease-induced mortality (ρ_i , $i = 1, 2$), but the effects of these variations on pathogen interactions will be discussed later (we set $\mu = 0.02$ and $\rho_i = 0$, $i = 1, 2$, except where otherwise noted).

4.1. Interactions between two related pathogens (strains)

For the case of two strains, we assume that the epidemiological characteristics of each strain are the same, so that one set of our baseline parameters applies to both strains (for illustration, we use measles). In Fig. 2, we compare the following three case studies motivated by possible antigenic strain interactions:

- (a) temporary symmetric cross-immunity/enhancement between strains;
- (b) temporary complete cross-immunity followed by continued symmetric cross-immunity/enhancement between strains;
- (c) permanent symmetric cross-immunity/enhancement between strains.

For (a) and (b), we simultaneously vary the average length of the period of temporary cross-immunity. For (c), we covary the basic reproductive ratio of the strains. We find that a temporary period of cross-enhancement can destabilize the equilibrium, leading to synchronous cycles in strain dynamics (Fig. 2a) in a similar manner to permanent enhancement (Ferguson et al., 1999) (Fig. 2c), even for average periods of a few days. As the strength and duration of cross-enhancement increases the dynamics become chaotic (not shown). However, if there is a short-lived period of cross-immunity before enhancement occurs (of at least 3 weeks), as is thought to be the case for dengue serotypes (Wearing and Rohani, 2006), then synchrony is lost and the pathogens cycle out-of-phase with each other (Fig. 2b). Permanent symmetric (partial) cross-immunity has previously been shown to produce stable dynamics independent of R_0 (Kamo and Sasaki, 2002) and this is reproduced in Fig. 2c. However, if partial cross-immunity is assumed to be temporary or follows a period of complete

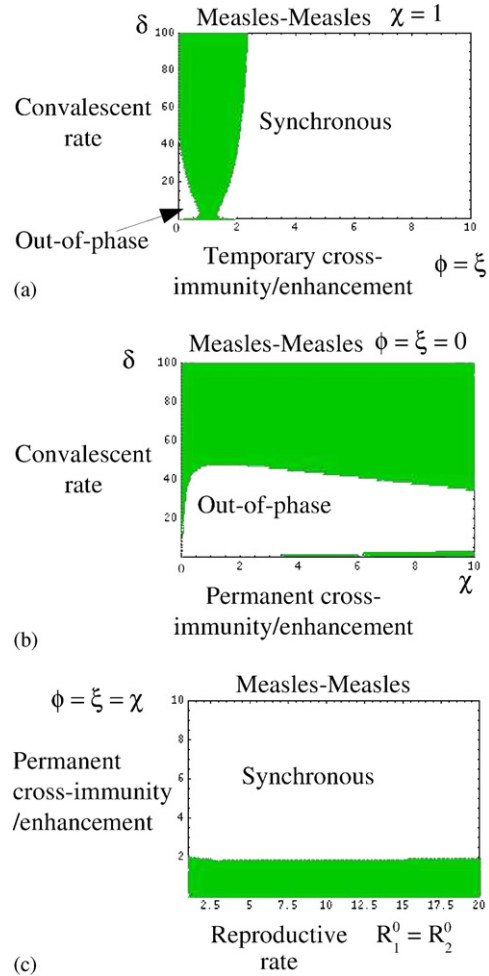


Fig. 2. Stability diagrams of different epidemiological scenarios for related strains. The gray region corresponds to a stable coexistence equilibrium. White regions are unstable and correspond to either stable antiphase or synchronous limit cycles: (a) temporary symmetric immunity/enhancement between strains; (b) temporary cross-immunity followed by continued symmetric immunity/enhancement between strains; (c) permanent symmetric cross-immunity/enhancement between strains. The baseline epidemic parameter set is that given for measles in Table 2. Note that in all figures, the units of δ are yr⁻¹.

cross-immunity, then sustained asynchronous oscillations can arise (Figs. 2a and b).

4.2. Interactions between two unrelated pathogens

For the case of two unrelated pathogens, we assume that the epidemiological characteristics of each infection are different. We also consider two different sets of disease parameters: one where the diseases share the same R_0 but have different infectious periods (measles–pertussis) and one where the diseases have different R_0 's and different infectious periods (measles–rubella). In this manner, and in tandem with the results of the previous section, we can detect the changes in pathogen interaction due to differences between the lengths of the infectious period,

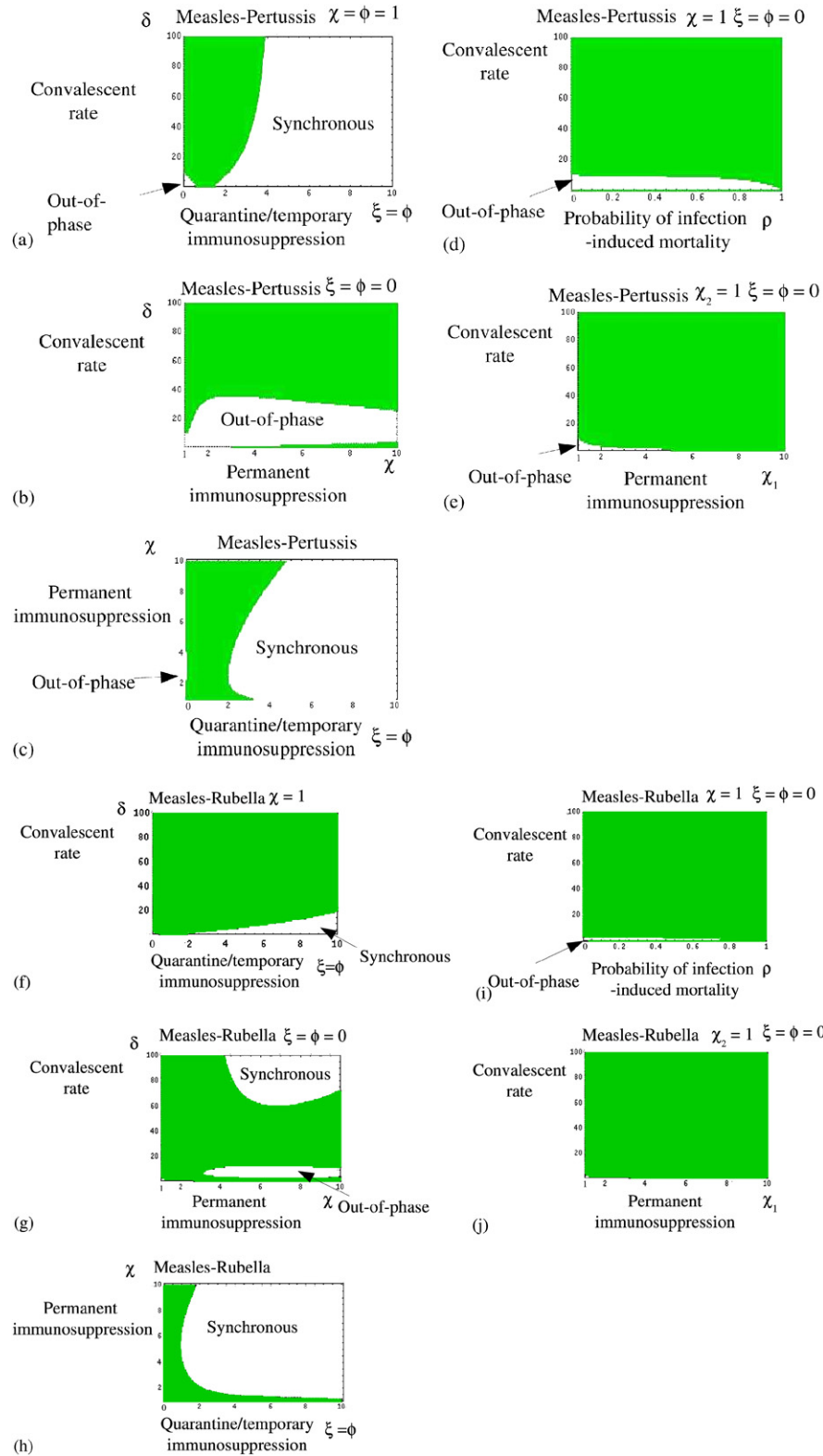


Fig. 3. Stability diagrams of different epidemiological scenarios for unrelated pathogens. The gray region corresponds to a stable coexistence equilibrium. White regions are unstable and correspond to either stable out-of-phase or synchronous attractors: (a) and (f) quarantine/temporary immunosuppression between diseases; (b) and (g) quarantine followed by permanent immunosuppression; (c) and (h) quarantine/temporary immunosuppression followed by permanent immunosuppression between diseases; (d) and (i) quarantine followed by infection-induced mortality; (e) and (j) quarantine followed by permanent asymmetric immunosuppression. The baseline epidemic parameter sets are given in Table 2.

and those due solely to differences between values of R_0 . In Fig. 3, we compare the following five case studies:

- (a) quarantine/temporary immunosuppression between diseases;
- (b) quarantine followed by permanent immunosuppression;
- (c) quarantine/temporary immunosuppression followed by permanent immunosuppression between diseases;
- (d) quarantine followed by infection-induced mortality;
- (e) quarantine followed by permanent asymmetric immunosuppression.

In each investigation we assume that the coinfection parameter (ϕ) is equal to the quarantine/temporary immunosuppression parameter (ξ) to allow for direct comparisons with results from the previous section. However, if ϕ is set equal to 1, representing the null position of non-interacting coinfection, then similar qualitative results are obtained although the regions of instability tend to be smaller.

Our analysis of the effects of quarantine and temporary immunosuppression on the dynamics of unrelated diseases shows similar results to those of cross-immunity and enhancement on strain dynamics. Figs. 2a, 3a and f, all share similar qualitative features: quarantine/cross-immunity periods longer than a certain amount of time lead to sustained out-of-phase cycles, whereas temporary immunosuppression/enhancement leads to sustained synchronous cycles. The major difference is that the unrelated pathogens with asymmetric infection parameters generate smaller regions of instabilities, in particular the pathogens with very different R_0 's (measles–rubella). Moreover, the length of quarantine required to achieve sustained cycles (with $\xi = \phi < 1$) in the unrelated pathogens is much longer than is realistic for many diseases.

If we assume short periods of quarantine and examine how immunosuppression following these periods affects the dynamics, then we find a substantial difference between the diagram for measles–pertussis (Fig. 3b) compared with that for measles–rubella (Fig. 3g). The interaction between unrelated pathogens with similar R_0 's but different infectious periods (measles–pertussis) closely resembles that for related pathogens with identical parameters (measles–measles, Fig. 2b). The interaction between unrelated pathogens with different R_0 's (measles–rubella) shows that for relatively short periods of quarantine, permanent immunosuppression can give rise to sustained synchronous cycles; asynchronous cycles only occur for much longer periods of quarantine. This difference is partially explained by considering Figs. 3c and h, in which we simultaneously vary the quarantine/temporary immunosuppression parameter with the permanent immunosuppression parameter. The unrelated pathogens with very different R_0 's (measles–rubella) interact to produce synchronous cycles over a much larger area of parameter space. We might infer from this that pathogens with similar

R_0 's are more susceptible to competition induced by a period of quarantine. This key difference is also demonstrated in Figs. 3d and i, in which we vary the probability of infection-induced mortality against the period of quarantine. We can see that mortality only has a significant effect on stability if the convalescent period is also long, but this region is much larger for measles–pertussis than measles–rubella. Again, asynchronous cycles are easier to induce in the unrelated pathogens with similar R_0 's.

Until this point, we have assumed that the interaction parameters have been symmetric, i.e. the same for both unrelated pathogens. Figs. 3e and j illustrate the effect of assuming that immunosuppression following quarantine occurs for only one of the two pathogens. Interestingly, in both cases, almost all the unstable regions observed in Figs. 3b and g become stable.

In summary, although we observe a range of behavior varying a suite of immunological and ecological parameters, there are two opposing mechanisms that drive the underlying dynamics: competition and cooperation. Cross-immunity, quarantine or disease-induced mortality create competition for the pool of susceptibles, of which the dynamical consequence is a temporal separation of outbreaks of each pathogen. Conversely, cross-enhancement and immunosuppression lead to facilitation between pathogens: infection with one strain or disease increases an individual's chance of contracting the second and thus epidemics are more likely to coincide. These observations give us a very intuitive signature of interaction: competitive mechanisms lead to out-of-phase dynamics, cooperative mechanisms lead to synchronous dynamics. However, the mechanisms do not always generate sustained cyclic dynamics and when they are acting together, for example when there is a period of quarantine/cross-immunity prior to enhancement/immunosuppression, then one (competition) seems to dominate the other.

In this section, we have focused on the stability of the coexistence equilibrium and the phase of the cyclic dynamics, but cycle period may also provide a key interaction signature. In the next section, we pursue a more rigorous examination of a subset of the analyses presented here.

5. Period and phase of attractors in two-pathogen epidemics

We now investigate the properties of period and phase, which characterize oscillations of the coexistence attractor. This allows us to explore how ecological and immune-mediated processes determine disease-specific dynamical outcomes. We show that the interaction of two principal eigenmodes (eigenvalue–eigenvector pairs) determines the dynamical outcome of our model. Instability of the coexistence equilibrium is generated when the real part of the eigenvalue from one of these pairs moves from being negative to positive across the imaginary axis, leading to a Hopf bifurcation. Depending upon how the eigenmode interactions generate the instability, the periodic attractors

may be either in-phase or out-of-phase. Thus, disease interactions may be tracked by continuously following the magnitude and direction of the two eigenmodes in parameter space. Our computational results demonstrate how ecological and immune-mediated processes may couple the amplitude and frequency components of two complex eigenmodes of our model. Although it is clear that in a 14-dimensional model many other eigenmode interactions are possible, we focus on the two complex pairs that appear to dominate the dynamic stability of the system. These two pairs were determined by performing a combination of extensive numerical exploration of the parameter space underlying the model and model simplification and mathematical analysis. The model simplification involves lumping several transient classes into one so that the state-space dimension reduces from 14 to 7. Approximate analytic results can then be obtained that allow better understanding the observed dynamics of the higher dimensional model.

Due to the complexity of our model we chose two analyses from the previous section to demonstrate this mechanism:

- (a) permanent symmetric cross-immunity/enhancement between strains;
- (b) quarantine followed by permanent immunosuppression between diseases.

5.1. Determinants of attractor properties

Of the 14 eigenvalues determined by the Jacobian of Eqs. (1) five principally determine the stability properties of the attractors studied in this paper. One of these is always real and is determined by the host lifetime μ^{-1} . The others are two pairs of complex eigenvalues. These are coupled by immune-mediated parameters ($\chi_i, \phi_i, \xi_i, \eta_i, i = 1, 2$) and their interactions with the epidemiological parameters ($\mu, \gamma_i, \sigma_i, \delta_i, i = 1, 2$). Since our model decouples into two independent epidemiological models when $\chi_i = \phi_i = \xi_i = \eta_i = 1$ the eigenmode interaction disappears at this point. We designate these two eigenmode (eigenvalue, eigenvector) pairs as (θ_1, v_1) and (θ_2, v_2) . Throughout this section the eigenmodes will be labeled in the graphs as red and blue colors, respectively, unless otherwise noted.

We now reduce the general model to the special case of two interacting strains, in which the classes E_i, I_i, C_i, S_i are collapsed into a single class, X_i (see Appendix C). The state of the resulting model takes the form $(S_0, X_1, X_2, \varepsilon_1, \varepsilon_2, \lambda_1, \lambda_2)$, where each of the remaining five state variables represents the same quantity corresponding to its value in Eqs. (1). As stated in Section 2 this reduces our model to one similar to that studied previously by Kamo and Sasaki (2002). Symmetrizing this reduced class of models it can be shown that the periods and phases of a stable periodic attractor are principally determined by two

dominant coupled eigenmodes, with eigenvalues,

$$\theta_1 \approx -\frac{(2-\phi)\mu \frac{R_0(\gamma+\mu)(\sigma+\mu)}{\sigma}}{2\gamma} + i\left(\frac{R_0(\gamma+\mu)(\sigma+\mu)}{\sigma}\mu\right)^{1/2}, \tag{4}$$

$$\theta_2 \approx -\frac{\phi\mu \frac{R_0(\gamma+\mu)(\sigma+\mu)}{\sigma}}{2\gamma} + i\left(\phi \frac{R_0(\gamma+\mu)(\sigma+\mu)}{\sigma}\mu\right)^{1/2} \tag{5}$$

if $\phi < 1$ and

$$\theta_1 \approx -\frac{\phi\mu \frac{R_0(\gamma+\mu)(\sigma+\mu)}{\sigma}}{2\gamma} + i\left(\phi \frac{R_0(\gamma+\mu)(\sigma+\mu)}{\sigma}\mu\right)^{1/2}, \tag{6}$$

$$\theta_2 \approx -\frac{(2-\phi)\mu \frac{R_0(\gamma+\mu)(\sigma+\mu)}{\sigma}}{2\gamma} + i\left(\frac{R_0(\gamma+\mu)(\sigma+\mu)}{\sigma}\mu\right)^{1/2} \tag{7}$$

if $\phi > 1$. In other words, $\theta_1 \rightarrow \theta_2$ and $\theta_2 \rightarrow \theta_1$ if $\phi > 1$ and the reverse occurs if $\phi < 1$. Eqs. (4) and (5) were derived previously by Kamo and Sasaki (2002) for the case $0 < \phi < 1$. Their analysis of model equilibria was restricted to the cross-immunity case and the equilibria they examined are not defined when $\phi > 1$ or the special cases $\phi = 0$ and 1. Nonetheless, their two-epidemic model decouples into two independent epidemics in the same way that ours does when $\phi = 1$ and all their results for the case $0 < \phi < 1$ can be used as benchmarks for the reduced symmetric case we analyse in this section. Future work, that is beyond the scope of the present paper, should allow showing that several of the results we state in the rest of this section also apply in some form, to the models developed by Gupta et al. (1998) and Ferguson et al. (1999). We showed earlier (see Fig. 2c) that for this class of models, when $\phi > 2$ the system spontaneously erupts into a stable periodic synchronous attractor. One can approximately compute the dominant interepidemic period for the attractor from the imaginary parts (eigenfrequencies) of one of the two dominant eigenmodes:

$$T_I^* = \frac{2\pi}{\text{Im}(\theta_i)}, \tag{8}$$

where $*$ represents the dominant eigenmode propagating through the attractor. Which mode dominates the periodicity properties of the attractor depends in a complex way upon the types of biological interactions and forcing mechanisms acting upon the system. We examine several examples in Sections 5.2 and 5.3.

Phase of a periodic attractor for our system can be studied by using the associated eigenvectors ($v_i, i = 1, 2$) corresponding to Eqs. (4)–(7). Each v_i has components that represent the seven state variables $(S_0, X_1, X_2, \varepsilon_1, \varepsilon_2, \lambda_1, \lambda_2)$. Since we are studying a symmetrized two-strain model we can write pairs of components (for example, X_1, X_2) of

each eigenvector as a ratio,

$$\frac{X_1}{X_2} = \frac{r_1 e^{i\Omega_1}}{r_2 e^{i\Omega_2}} = \frac{r_1}{r_2} e^{i(\Omega_1 - \Omega_2)} = \frac{r_1}{r_2} e^{i(\Delta\Omega)}, \quad (9)$$

where $r_i = (a_i^2 + b_i^2)$ is the magnitude of the complex eigenvalue θ_i with $a_i = \text{Re}(\theta_i)$, $b_i = \text{Im}(\theta_i)$; Ω_i is the phase angle in the complex plane and is equal to $\tan^{-1}(b_i/a_i)$ and $\Delta\Omega = \Omega_1 - \Omega_2$, the phase difference between infected trajectories of the two strains. For these definitions the two strains exhibit an in-phase attractor if $\Delta\Omega = 0$ and an out-of-phase (or antiphase) periodic attractor if $\Delta\Omega = \pi$. Thus, each of the eigenmodes represents a in-phase and an out-of-phase signature of a periodic attractor. According to Eqs. (4)–(7) the two eigenmode signatures will exhibit a switch, depending on whether $\phi < 1$ or $\phi > 1$. Thus, whether an eigenmode exhibits an in-phase or out-of-phase signature is determined by the immune-mediation parameter ϕ . Analysis of the entire eigensystem shows that there exists an eigenphase that synchronizes and desynchronizes the dynamical system as its eigensystem rotates by π radians.

5.2. Permanent symmetric immune-interaction between strains

We now explore how the effects of permanent cross-immunity ($\phi < 1$) and facilitation ($\phi > 1$) determine unique phase signatures for the reduced symmetric two-strain

model. The results are shown in Fig. 4. Fig. 4a shows how the predicted period changes as a function of the R_0 's and the cross-immunity/enhancement parameter $\phi = \xi = \chi$. Our reduced model predicts that with cross-immunity $\phi = \xi = \chi = 0.8$ we would obtain a pair of attractors, one determined by a synchronous eigenvalue (the blue surface) and one determined by an out-of-phase eigenvalue (the red surface) both with period 2. As the system increases the intensity of cross-immunity to $\phi = \xi = \chi = 0.2$ our model predicts a period 8 out-of-phase attractor.

For the case $\phi = \xi = \chi > 1$ we examine the onset of a synchronous limit cycle as $\phi = \xi = \chi > 2$. Fig. 4b shows that this limit cycle occurs as a result of a Hopf bifurcation arising from the same eigenvalue that resulted in the out-of-phase attractor in the case of cross-immunity. This eigenvalue switching was predicted earlier by Eqs. (4)–(7). Fig. 4c shows this phase switching as a function of R_0 by numerically computing the components of the eigenvectors (Eq. (9)) corresponding to the dominant eigenvalues.

5.3. Quarantine followed by permanent immunosuppression

As shown previously in Fig. 1 and discussed in Section 3, immunosuppression can lead to facilitation between unrelated pathogens, whereby one pathogen can increase the likelihood of persistence with another. We also demonstrated in Section 4.2 that reducing the convalescent

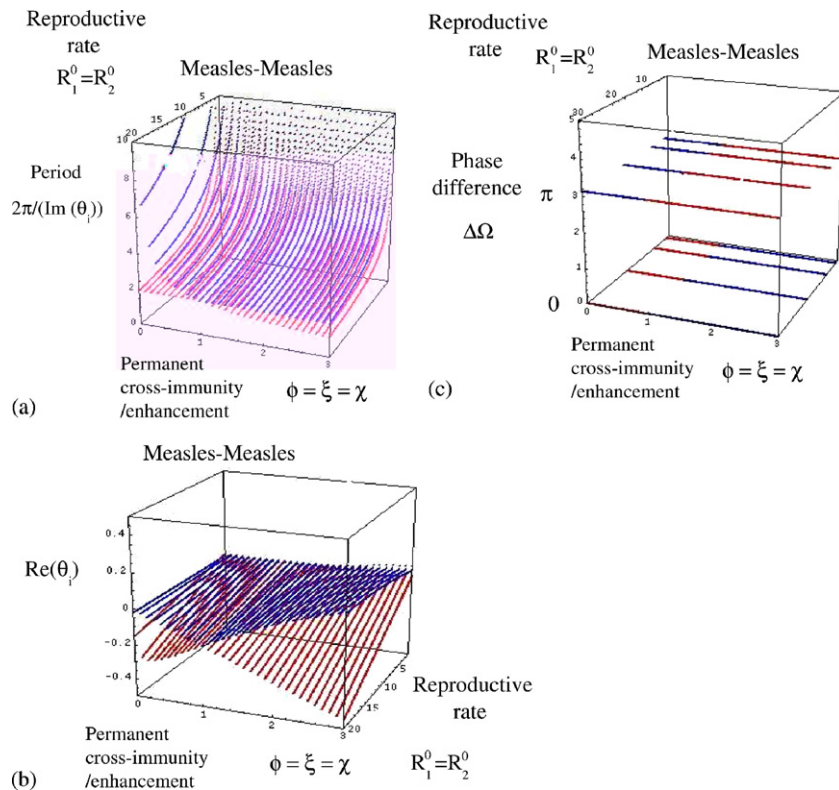


Fig. 4. Scenario for temporary symmetric immune-mediated measles–measles interactions: (a) interepidemic periods computed from imaginary parts of two eigenvalues (period = $2\pi/\text{Im}(\theta_i)$), versus $(R_0, \phi = \xi = \chi)$ parameter space; (b) real parts of two eigenvalues ($\text{Re}(\theta_i)$) versus $(R_0, \phi = \xi = \chi)$ parameter space; (c) phase differences of (X_1, X_2) components of two complex eigenvectors (v_i) versus $(R_0, \phi = \xi = \chi)$ parameter space.

period can modulate the re-infection effect by further reducing competition for susceptibles. Conversely, by increasing the convalescent period, and making convalescent individuals less likely to be available for re-infection, this parameter can enhance competition. These results were obtained assuming a period of complete quarantine ($\phi = \xi = 0$), but Fig. 5 shows that each of these effects has a unique disease interaction signature which is still present in the null case ($\phi = \xi = 1$). While both the measles–pertussis and measles–rubella scenarios show significant regions of synchronous and asynchronous attractors in parameter space, the relative size of these regions varies. In general, however, decreasing the convalescent period with increasing immunosuppression leads to synchronous cycling, whereas increasing the convalescent period leads to out-of-phase attractors. The major role of the convalescent class is to delay the onset of the permanent immunosuppressive effect: thus, the degree of facilitation between pathogens is significantly modulated by this delay.

Intuitively, we would expect that decreasing the birth rate should increase the intensity of competition between diseases for the pool of susceptibles, since it is replenished at a slower rate. Fig. 5b shows that increasing the birth rate (from $\mu = 0.01$ to 0.02) causes the synchronous region to disappear for the measles–pertussis scenario. Conversely, for the measles–rubella scenario, increasing the birth rate causes the out-of-phase region to disappear (Fig. 5d). Thus, increasing the birth rate for diseases with very different R_0 's (measles–rubella) appears to increase the effects of facilitation but decrease those of interference: the opposite of what occurs for diseases with similar R_0 's (measles–pertussis). Such diseases may experience higher competition for the pool of susceptibles. Fig. 5f shows that the real parts of two complex pairs of eigenvalues exhibit two distinct phase signatures depending on whether diseases are showing interference or facilitation. In Fig. 5f the real part of the eigenvalue θ_1 (represented as the red surface) loses stability and gives rise to stable synchronous attractors. The real part of the eigenvalue θ_2 (represented as the blue surface) loses stability to give rise to regions of *both* stable in-phase and out-of-phase attractors.

Fig. 5e shows that the eigenfrequency (imaginary part) of the eigenvalue θ_2 (represented as the blue surface) is sensitive to permanent immunosuppression while the eigenfrequency of the eigenvalue θ_1 is relatively insensitive unless $\chi < 1$ (which would represent some form of permanent quarantine between the two diseases). Inspection of Fig. 5e demonstrates that the sensitive eigenfrequency of this complex pair determines the expected dominant period of the time series. Unless the convalescent period becomes very long (i.e. δ becomes very small) both eigenfrequencies remain almost stationary over the part of parameter space we consider. Table 2 gives the intrinsic epidemiological periods (T_I) of measles, pertussis and rubella, which are computed using the baseline parameters listed in the table. The intrinsic period for uncoupled

epidemics is approximately two years for both measles and pertussis. Using our computational results it is now possible to explore the effects of immunoeological interactions in modulating the intrinsic period of the coupled epidemic time series via interaction of the two principal eigenmodes, as shown in Fig. 5g.

The boldface letters *A*, *B* and *C* in Fig. 5a designate the regions in (δ, χ) parameter space in which eigenvalue interactions between θ_1 and θ_2 modulate the dynamical outcomes. Thus, at point *A* our theory predicts an intrinsic period of the coupled time series with period 3.3 yr in-phase cycles. The observed period of 3.3 yr in the time series generated by numerical integration of the full system (Fig. 6c) bears out this prediction. At point *B* of Fig. 5a our theory predicts an intrinsic period of the coupled time series with period 1.5 yr out-of-phase cycles. Again, Fig. 6b shows that the period 1.6 is close to what we observe in the corresponding solution of the full system. At point *C* of Fig. 5a our theory predicts an intrinsic period of the coupled time series with 3.3 yr in-phase cycles. Time series with a period 3.3 yr in-phase cycling are presented in Fig. 6a. Fig. 6d shows that the eigenvalue value interaction surfaces also determine the maximum amplitude of the cycles. As the real part of the dominant eigenvalue passes through zero and continues to increase through (δ, χ) parameter space, the amplitude associated with the dominant eigenvalue also increases.

6. Conclusions and discussion

The mathematical model we develop in this paper will allow investigators to gain a better understanding of currently available extensive data sets that have accumulated from case report data with respect to multi-pathogen epidemics. Thus, we are now in a better position to address the potential benefits and pitfalls that may arise from using mechanistic models of multi-pathogen epidemics to develop robust statistical methodologies. Our framework also allows the systematic exploration of public health implications arising from interactions between pathogens. Hence, it may present a novel way of understanding prediction and forecasting of multi-pathogen interacting epidemics in disease communities.

There are several advantages of mechanistic modeling of multi-pathogen epidemics. One significant advantage is that specified mechanisms of disease transmission and spread can be precisely stated and analysed. Our model adds to previous work on mechanistic modeling disease strain interactions (Elveback et al., 1968; Dietz, 1979; White et al., 1998; Gog et al., 2002; Kamo and Sasaki, 2002; Abu-Raddad and Ferguson, 2004). With respect to incorporation of immune-mediated processes in two disease models, we considered the additional problem of mechanistically distinguishing between related and unrelated pathogens. In our model we have started as simply as possible. We model the immune-mediated processes in our model in terms of three parameters χ , ϕ , ξ (for simplicity of

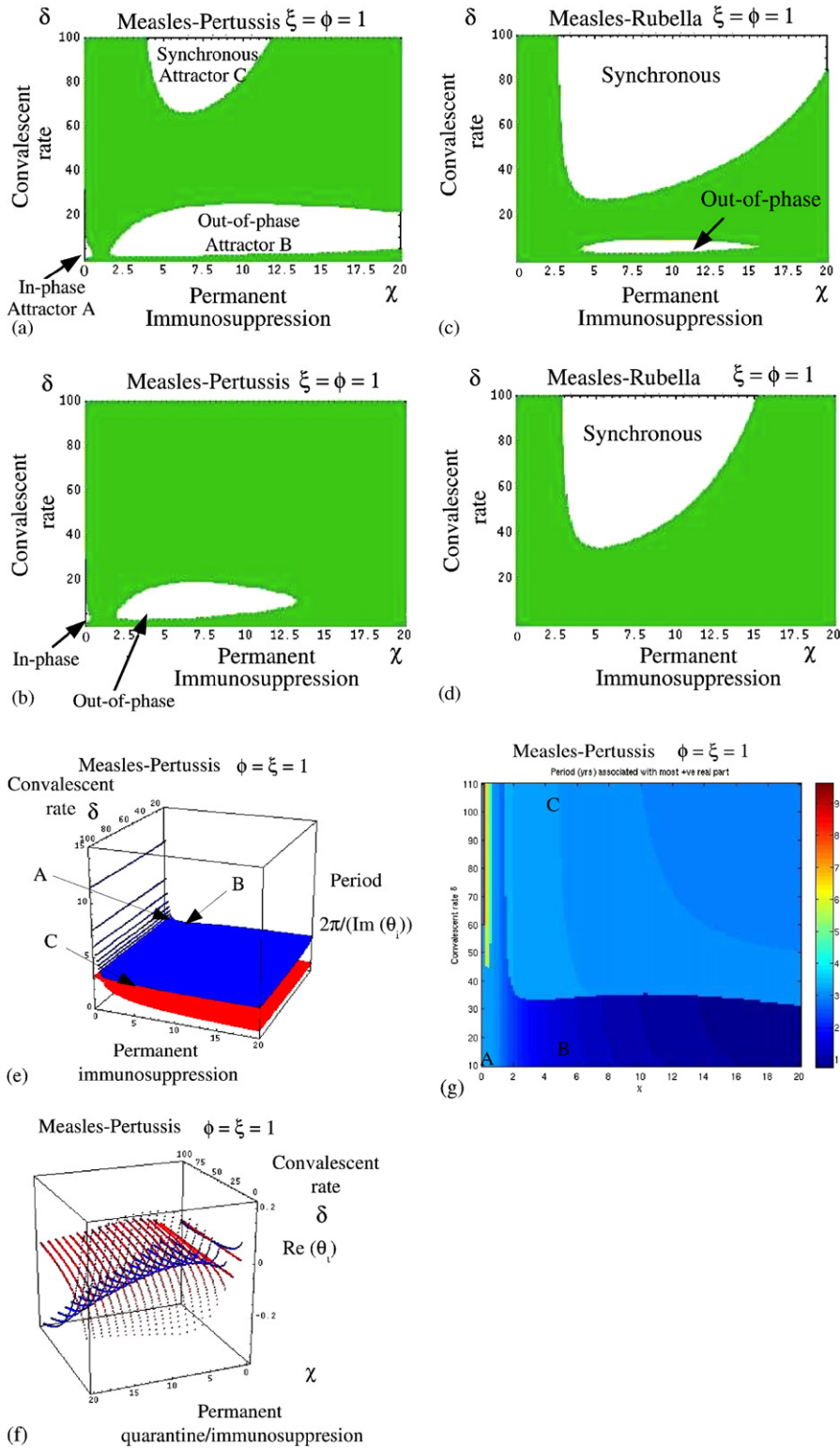


Fig. 5. Stability diagrams of different epidemiological scenarios for unrelated pathogens. The gray region corresponds to a stable coexistence equilibrium. White regions are unstable coexistence equilibrium points and correspond to either stable out-of-phase or synchronous attractors. (a) measles–pertussis interaction with low birth rate ($\mu = 0.01$); (b) measles–pertussis interaction with standard birth rate ($\mu = 0.02$); (c) measles–rubella interaction with low birth rate ($\mu = 0.01$); (d) measles–rubella interaction with standard birth rate ($\mu = 0.02$); (e) plots of the interepidemic periods computed from imaginary parts of two eigenvalues (period = $2\pi/\text{Im}(\theta_i)$), for (δ, χ) parameter space; (f) plots of the real parts of two eigenvalues ($\text{Re}(\theta_i)$) in (δ, χ) , for measles–pertussis interaction; (g) contour plot showing how the period varies for the in-phase and out-of-phase attractors A, B and C regions. The baseline epidemic parameter sets are given in Table 2.

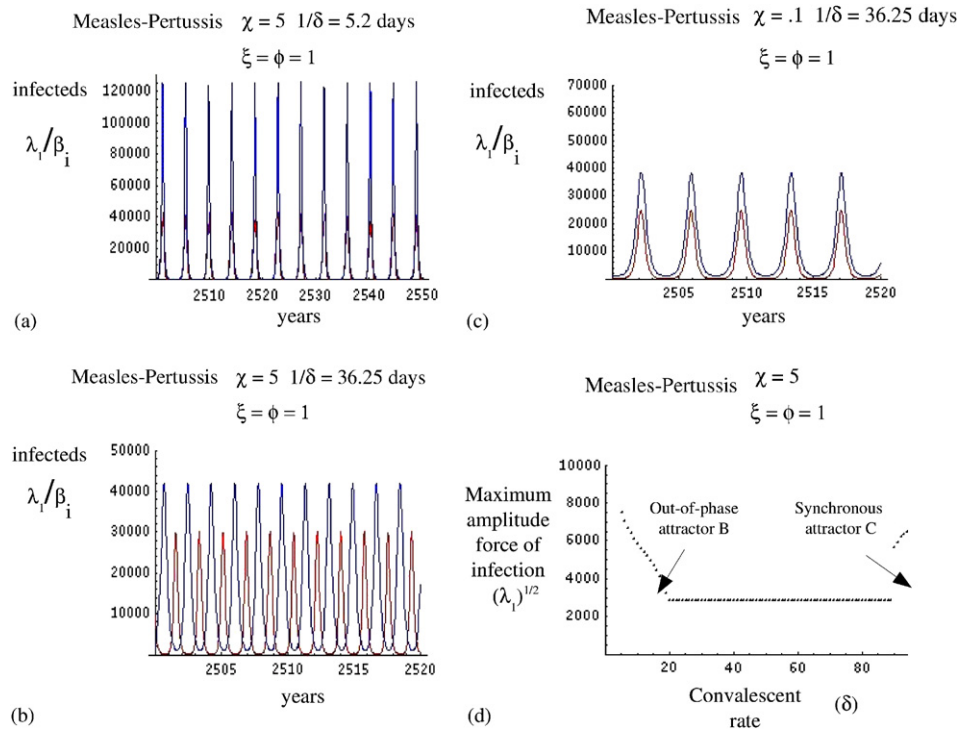


Fig. 6. Each panel illustrates summary properties characteristic of the two-disease time series: amplitude, phase and period of coupled oscillations. In this paper we use these summary properties to mine disease-specific interference or facilitation signatures out of immunoeological interactions. To generate these time series a measles–pertussis interaction scenario was assumed. The baseline epidemic parameter sets are given in Table 2: (a) synchronous (in-phase) infected time series with low birth rate ($\mu = 0.01$), short convalescence ($1/\delta = 5.2$ days) and large permanent immunosuppression effect ($\chi = 5$); (b) out-of-phase infected time series with low birth rate ($\mu = 0.01$), long convalescence ($1/\delta = 36.25$ days) and large permanent immunosuppression ($\chi = 5$); (c) synchronous (in-phase) infected time series with low birth rate ($\mu = 0.01$), long convalescence ($1/\delta = 36.25$ days) and permanent quarantine effect ($\chi = 0.1$); (d) amplitude-response as measured by the maximum amplitude of square-root of force of infection for measles plotted versus convalescent rate. Out-of-phase attractors show increasing amplitude as convalescent rate decreases. Synchronous attractors show increasing amplitude as convalescent rate increases. The parameters determining the time series (a)–(c) of this figure are points of (χ, δ) parameter spaces shown in Fig. 5 from the regions labeled attractors C, B and A, respectively. Also see Fig. 5 with corresponding exposition in the text describing how eigenmode interactions generate oscillatory instabilities and attractor properties.

exposition, we assume here symmetry between the immune-mediated parameters). Each of these are distinguished by the permanency or temporary action of the immune response in mediating the transmission and spread of disease. The parameter χ represents the effect of permanent cross-immunity (or removal/quarantine) when it is less than one and immunosuppression when it is greater than one. The parameters ϕ and ξ represent temporary cross-immunity (or removal/quarantine) or immunosuppression. With this parameterization we were able to distinguish immune-mediated effects between related strains versus unrelated pathogens. Although simple, this parameterization allowed us to distinguish model mechanisms and infer their dynamical effects. In our approach, depending upon how these three parameters are specified in the model, we were able to add complexity one step at a time so that the dynamical effects of key mechanisms could be identified. This proved to be particularly important in distinguishing between the interaction signatures arising from oscillatory instabilities in related strains versus unrelated pathogens.

A second advantage is the introduction of key ecological interactions into multi-pathogen epidemics. Previous work

has demonstrated the importance of introducing ecological mechanisms for interaction, such as convalescence and disease-induced mortality (Rohani et al., 1998, 2003; Huang and Rohani, 2005, 2006). Our model simultaneously incorporates both ecological and immune-mediated processes so that a comprehensive comparison between these processes could be performed. Thus, our model may permit the exploration of how covariation of ecological and immune-mediated effects may produce unique dynamical interaction signatures. One last advantage of our mechanistic approach is that the interaction parameters are hierarchically incorporated or nested within the dynamical equations. For example, if we want to examine the null hypothesis that diseases do not interact then we may assert that $\chi = \phi = \xi = 1$. This is equivalent to assuming that the dynamical system decouples into two independent epidemics. If we want to test the hypothesis that permanent or temporary cross-immunity does not exist between two unrelated pathogens then we may assert that $(\chi \geq 1, \phi \geq 1, \xi \geq 1)$ must hold in the parameter space for this case. For each of these cases we have shown that there are clear dynamical consequences associated with each assertion.

While work is just beginning on the construction of models general enough to incorporate realistic and immune-mediated processes into multi-pathogen interactions, the prognosis for progress is a good one. Combined with disease-specific scenario modeling and a strong database, a predictive theory of multi-pathogen epidemics is now on the horizon.

Acknowledgments

We thank an anonymous reviewer for their careful comments on this paper. This work was funded by grants from the National Science Foundation (DEB-0343176), the National Institutes of Health (1R01GM069111-01A1) and the Ellison Medical Foundation to PR.

Appendix A

In this appendix, we provide the full equations tracking the entire immune history of a general two-pathogen single-host system. The equations we present in this appendix would be used when developing a stochastic analogue of the system, while the reduced system of equations (1), are more conducive to an investigation of deterministic dynamics, as has been carried out in this paper.

First, we define the state variables X_{ij} by their subscripts, which track status with regards to each pathogen: i denotes infection status (susceptible, exposed, infectious, convalescent or recovered) with respect to pathogen 1 and j denotes infection status with respect to pathogen 2.

$$\frac{dX_{SS}}{dt} = vN - (\lambda_1 + \lambda_2) \frac{X_{SS}}{N} - \mu X_{SS}, \quad (\text{A.1})$$

$$\frac{dX_{ES}}{dt} = \lambda_1 \frac{X_{SS}}{N} - \phi_2 \lambda_2 \frac{X_{ES}}{N} - (\sigma_1 + \mu) X_{ES}, \quad (\text{A.2})$$

$$\frac{dX_{IS}}{dt} = \sigma_1 X_{ES} - \phi_2 \lambda_2 \frac{X_{IS}}{N} - (\gamma_1 + \mu) X_{IS}, \quad (\text{A.3})$$

$$\frac{dX_{CS}}{dt} = \gamma_1 X_{IS} - \xi_2 \lambda_2 \frac{X_{CS}}{N} - (\delta_1 + \mu) X_{CS}, \quad (\text{A.4})$$

$$\frac{dX_{RS}}{dt} = (1 - \rho_1) \delta_1 X_{CS} - \chi_2 \lambda_2 \frac{X_{RS}}{N} - \mu X_{RS}, \quad (\text{A.5})$$

$$\frac{dX_{SE}}{dt} = \lambda_2 \frac{X_{SS}}{N} - \phi_1 \lambda_1 \frac{X_{SE}}{N} - (\sigma_2 + \mu) X_{SE}, \quad (\text{A.6})$$

$$\frac{dX_{SI}}{dt} = \sigma_2 X_{SE} - \phi_1 \lambda_1 \frac{X_{SI}}{N} - (\gamma_2 + \mu) X_{SI}, \quad (\text{A.7})$$

$$\frac{dX_{SC}}{dt} = \gamma_2 X_{SI} - \xi_1 \lambda_1 \frac{X_{SC}}{N} - (\delta_2 + \mu) X_{SC}, \quad (\text{A.8})$$

$$\frac{dX_{SR}}{dt} = (1 - \rho_2) \delta_2 X_{SC} - \chi_1 \lambda_1 \frac{X_{SR}}{N} - \mu X_{SR}, \quad (\text{A.9})$$

$$\frac{dX_{EE}}{dt} = \phi_2 \lambda_2 \frac{X_{ES}}{N} + \phi_1 \lambda_1 \frac{X_{SE}}{N} - (\sigma_1 + \sigma_2 + \mu) X_{EE}, \quad (\text{A.10})$$

$$\frac{dX_{IE}}{dt} = \sigma_1 X_{EE} + \phi_2 \lambda_2 \frac{X_{IS}}{N} - (\sigma_2 + \gamma_1 + \mu) X_{IE}, \quad (\text{A.11})$$

$$\frac{dX_{CE}}{dt} = \gamma_1 X_{IE} + \xi_2 \lambda_2 \frac{X_{CS}}{N} - (\sigma_2 + \delta_1 + \mu) X_{CE}, \quad (\text{A.12})$$

$$\frac{dX_{RE}}{dt} = (1 - \rho_1) \delta_1 X_{CE} + \chi_2 \lambda_2 \frac{X_{RS}}{N} - (\sigma_2 + \mu) X_{RE}, \quad (\text{A.13})$$

$$\frac{dX_{EI}}{dt} = \sigma_2 X_{EE} + \phi_1 \lambda_1 \frac{X_{SI}}{N} - (\sigma_1 + \gamma_2 + \mu) X_{EI}, \quad (\text{A.14})$$

$$\frac{dX_{EC}}{dt} = \gamma_2 X_{EI} + \xi_1 \lambda_1 \frac{X_{SC}}{N} - (\sigma_1 + \delta_2 + \mu) X_{EC}, \quad (\text{A.15})$$

$$\frac{dX_{ER}}{dt} = (1 - \rho_2) \delta_2 X_{EC} + \chi_1 \lambda_1 \frac{X_{SR}}{N} - (\sigma_1 + \mu) X_{ER}, \quad (\text{A.16})$$

$$\frac{dX_{II}}{dt} = \sigma_1 X_{EI} + \sigma_2 X_{IE} - (\gamma_1 + \gamma_2 + \mu) X_{II}, \quad (\text{A.17})$$

$$\frac{dX_{CI}}{dt} = \sigma_2 X_{CE} + \gamma_1 X_{II} - (\gamma_2 + \delta_1 + \mu) X_{CI}, \quad (\text{A.18})$$

$$\frac{dX_{RI}}{dt} = \sigma_2 X_{RE} + (1 - \rho_1) \delta_1 X_{CI} - (\gamma_2 + \mu) X_{RI}, \quad (\text{A.19})$$

$$\frac{dX_{IC}}{dt} = \sigma_1 X_{EC} + \gamma_2 X_{II} - (\gamma_1 + \delta_2 + \mu) X_{IC}, \quad (\text{A.20})$$

$$\frac{dX_{IR}}{dt} = \sigma_1 X_{ER} + (1 - \rho_2) \delta_2 X_{IC} - (\gamma_1 + \mu) X_{IR}, \quad (\text{A.21})$$

$$\frac{dX_{CC}}{dt} = \gamma_1 X_{IC} + \gamma_2 X_{CI} - (\delta_1 + \delta_2 + \mu) X_{CC}, \quad (\text{A.22})$$

$$\frac{dX_{RC}}{dt} = \gamma_2 X_{RI} + (1 - \rho_1) \delta_1 X_{CC} - (\delta_2 + \mu) X_{RC}, \quad (\text{A.23})$$

$$\frac{dX_{CR}}{dt} = \gamma_1 X_{IR} + (1 - \rho_2) \delta_2 X_{CC} - (\delta_1 + \mu) X_{CR}, \quad (\text{A.24})$$

$$\frac{dX_{RR}}{dt} = (1 - \rho_2) \delta_2 X_{RC} + (1 - \rho_1) \delta_1 X_{CR} - \mu X_{RR}, \quad (\text{A.25})$$

where $\lambda_1 = \beta_1(X_{IS} + X_{IE} + X_{II} + X_{IC} + X_{IR})$ and $\lambda_2 = \beta_2(X_{SI} + X_{EI} + X_{II} + X_{CI} + X_{RI})$ are the pathogen-specific forces of infection. Note that to incorporate the parameter η —which modulates infectiousness—into this framework requires additional compartments to keep track of the order in which individuals become infected. For ease of exposition, we do not present these here, however, we do describe how η is incorporated within the reduced framework below.

These equations reduce to the system of equations (1) in the following way:

- (i) Define $X_{ss} = S_0$, $X_{iS} = i_1$ and $X_{Sj} = j_2$ so that Eqs. (A.1)–(A.9) are exactly the first nine equations of (1).
- (ii) Also define $\varepsilon_1 = X_{ES} + X_{EE} + X_{EI} + X_{EC} + X_{ER}$ and $\varepsilon_2 = X_{SE} + X_{EE} + X_{IE} + X_{CE} + X_{RE}$, so that

$$\frac{d\varepsilon_1}{dt} = \lambda_1 \frac{S_0}{N} + \phi_1 \lambda_1 \frac{E_2 + I_2}{N} + \xi_1 \lambda_1 \frac{C_2}{N} + \chi_1 \lambda_1 \frac{S_2}{N} - \rho_2 \delta_2 X_{EC} - (\sigma_1 + \mu) \varepsilon_1,$$

$$\frac{d\varepsilon_2}{dt} = \lambda_2 \frac{S_0}{N} + \phi_2 \lambda_2 \frac{E_1 + I_1}{N} + \xi_2 \lambda_2 \frac{C_1}{N} + \chi_2 \lambda_2 \frac{S_1}{N} - \rho_1 \delta_1 X_{CE} - (\sigma_2 + \mu) \varepsilon_2,$$

$$\frac{d\lambda_1}{dt} = \beta_1 \sigma_1 \varepsilon_1 - \rho_2 \delta_2 X_{IC} - (\gamma_1 + \mu) \lambda_1,$$

$$\frac{d\lambda_2}{dt} = \beta_2 \sigma_2 \varepsilon_2 - \rho_1 \delta_1 X_{CI} - (\gamma_2 + \mu) \lambda_2.$$

When $\rho_1 \delta_1 X_{EC}$, $\rho_2 \delta_2 X_{CE}$, $\rho_1 \delta_1 X_{CI}$ and $\rho_2 \delta_2 X_{CI}$ are relatively small then these terms can be neglected and we obtain the equations given in (1) (with $\eta_1 = \eta_2 = 1$). Numerical investigation can be used to show that for the acute infections (those with “short” latent and infectious periods) examined in this paper, this approximation is reasonable. For chronic infections, disease-induced mortality is likely to occur whilst an individual is still infected and therefore an alternative representation is necessary. Of course, when there is no disease-induced mortality then this approximation is exact, but we note that it is also exact when $\phi_i = \xi_i = 0$, $i = 1, 2$.

- (iii) With this approximation, and since we assume that N remains constant even in the presence of disease-induced mortality, once individuals have been exposed to both pathogens it is no longer dynamically important to keep track of the final 16 variables (i.e. solve Eqs. (A.10)–(A.25) explicitly). We therefore lump all these states— X_{EE} through X_{RR} —into a single class, S_{12} . For short latent, infectious and convalescent classes (relative to the average life expectancy), the following equation is thus a reasonable approximation tracking those individuals who have been exposed to both pathogens and do not suffer disease-induced mortality:

$$\begin{aligned} \frac{dS_{12}}{dt} = & (1 - \rho_1)(1 - \rho_2) \left(\phi_2 \lambda_2 \frac{E_1 + I_1}{N} + \xi_2 \lambda_2 \frac{C_1}{N} \right. \\ & \left. + \phi_1 \lambda_1 \frac{E_2 + I_2}{N} + \xi_1 \lambda_1 \frac{C_2}{N} \right) \\ & + (1 - \rho_2) \chi_2 \lambda_2 \frac{S_1}{N} + (1 - \rho_1) \chi_1 \lambda_1 \frac{S_2}{N} - \mu S_{12}. \end{aligned}$$

This approximation discounts mortality earlier than it occurs and so slightly underestimates survival.

A.1. Incorporating η : the forces of latency (ε) and infection (λ)

We briefly describe how we can modify the reduced system to incorporate the parameter η . Let E_{iP} (I_{iP}) denote individuals exposed to (infected with) pathogen i as a primary infection and E_{iS} (I_{iS}) denote individuals exposed to (infected with) pathogen i as a secondary infection. Then

$$\frac{dE_{1P}}{dt} = \lambda_1 \frac{S_0}{N} - (\sigma_1 + \mu) E_{1P}, \tag{A.26}$$

$$\frac{dE_{2P}}{dt} = \lambda_2 \frac{S_0}{N} - (\sigma_2 + \mu) E_{2P}, \tag{A.27}$$

$$\begin{aligned} \frac{dE_{1S}}{dt} = & \phi_1 \lambda_1 \frac{E_2 + I_2}{N} + \xi_1 \lambda_1 \frac{C_2}{N} + \chi_1 \lambda_1 \frac{S_2}{N} \\ & - (\sigma_1 + \mu) E_{1S}, \end{aligned} \tag{A.28}$$

$$\begin{aligned} \frac{dE_{2S}}{dt} = & \phi_2 \lambda_2 \frac{E_1 + I_1}{N} + \xi_2 \lambda_2 \frac{C_1}{N} + \chi_2 \lambda_2 \frac{S_1}{N} \\ & - (\sigma_2 + \mu) E_{2S}, \end{aligned} \tag{A.29}$$

$$\frac{dI_{1P}}{dt} = \sigma_1 E_{1P} - (\gamma_1 + \mu) I_{1P}, \tag{A.30}$$

$$\frac{dI_{2P}}{dt} = \sigma_2 E_{2P} - (\gamma_2 + \mu) I_{2P}, \tag{A.31}$$

$$\frac{dI_{1S}}{dt} = \sigma_1 E_{1S} - (\gamma_1 + \mu) I_{1S}, \tag{A.32}$$

$$\frac{dI_{2S}}{dt} = \sigma_2 E_{2S} - (\gamma_2 + \mu) I_{2S} \tag{A.33}$$

and defining $\varepsilon_i = E_{iP} + \eta_i E_{iS}$ and $\lambda_i = \beta_i (I_{iP} + \eta_i I_{iS})$, $i = 1, 2$ we obtain the equations presented in (1).

Appendix B

In this appendix we state the equations used to numerically compute the equilibrium states, the Jacobian, and eigenvalues of the model specified by Eqs. (1). As mentioned in the main text, we note that N remains constant even in the presence of disease-induced mortality so that the state equation for dS_{12}/dt is uncoupled from the dynamical system. As it plays no role in determining the equilibrium of the other state variables it will therefore be ignored in this appendix.

First, determine each of the state variables as a function of the forces of infection (λ_1, λ_2),

$$\hat{S}_0 = \frac{\mu}{\hat{\lambda}_1 + \hat{\lambda}_2 + \mu},$$

$$\hat{E}_i = \left(\frac{\hat{\lambda}_i}{\phi_j \hat{\lambda}_j + \sigma_i + \mu} \right) \left(\frac{\mu}{\hat{\lambda}_1 + \hat{\lambda}_2 + \mu} \right),$$

$$\hat{I}_i = \left(\frac{\hat{\lambda}_i \sigma_i}{\phi_j \hat{\lambda}_j + \gamma_i + \mu} \right) \left(\frac{1}{\phi_j \hat{\lambda}_j + \sigma_i + \mu} \right) \left(\frac{\mu}{\hat{\lambda}_1 + \hat{\lambda}_2 + \mu} \right),$$

$$\hat{C}_i = \left(\frac{\hat{\lambda}_i \gamma_i}{\xi_j \hat{\lambda}_j + \delta_i + \mu} \right) \left(\frac{\sigma_i}{\phi_j \hat{\lambda}_j + \gamma_i + \mu} \right) \left(\frac{1}{\phi_j \hat{\lambda}_j + \sigma_i + \mu} \right) \times \left(\frac{\mu}{\hat{\lambda}_1 + \hat{\lambda}_2 + \mu} \right),$$

$$\hat{S}_i = \left(\frac{\hat{\lambda}_i (1 - \rho_i) \delta_i}{\chi_j \hat{\lambda}_j + \mu} \right) \left(\frac{\gamma_i}{\xi_j \hat{\lambda}_j + \delta_i + \mu} \right) \left(\frac{\sigma_i}{\phi_j \hat{\lambda}_j + \gamma_i + \mu} \right) \times \left(\frac{1}{\phi_j \hat{\lambda}_j + \sigma_i + \mu} \right) \left(\frac{\mu}{\hat{\lambda}_1 + \hat{\lambda}_2 + \mu} \right),$$

$$\hat{e}_i = (\hat{\lambda}_i \hat{S}_0 + \eta_i (\phi_i \hat{\lambda}_i \hat{E}_i + \phi_i \hat{\lambda}_i \hat{I}_i + \xi_i \hat{\lambda}_i \hat{C}_i + \chi_i \hat{\lambda}_i \hat{S}_i)) (\sigma_i + \mu)^{-1}, \quad (\text{B.1})$$

where the symbol $\hat{\cdot}$ represents the equilibrium value of the state variable scaled by N , and the indices i and j represent the equilibrium states for the disease i interacting with disease j (where i and j can take on the values 1, 2, with $i \neq j$). Equilibria of Eqs. (1) can now be computed as nonnegative solutions of the implicit equations:

$$\hat{\lambda}_i = \beta_i \sigma_i \hat{e}_i (\gamma_i + \mu)^{-1}. \quad (\text{B.2})$$

Appendix C

In this section we demonstrate the reduction of the 14-dimensional system to a seven-dimensional system and show how these two systems decouple into two single-disease models.

Assume that there is no disease-induced mortality for either disease, $\rho_1 = \rho_2 = 0$. Assume that $\chi_1 = \xi_1 = \phi_1$, $\chi_2 = \xi_2 = \phi_2$ and $\eta_1 = \eta_2 = 1$. Let $X_i = E_i + I_i + C_i + S_i$, $i = 1, 2$. Then

$$\frac{dS_0}{dt} = vN - (\lambda_1 + \lambda_2) \frac{S_0}{N} - \mu S_0, \quad (\text{C.1})$$

$$\frac{dX_1}{dt} = \lambda_1 \frac{S_0}{N} - \phi_2 \lambda_2 \frac{X_1}{N} - \mu X_1, \quad (\text{C.2})$$

$$\frac{dX_2}{dt} = \lambda_2 \frac{S_0}{N} - \phi_1 \lambda_1 \frac{X_2}{N} - \mu X_2, \quad (\text{C.3})$$

$$\frac{dS_{12}}{dt} = \phi_2 \lambda_2 \frac{X_1}{N} + \phi_1 \lambda_1 \frac{X_2}{N} - \mu S_{12}, \quad (\text{C.4})$$

$$\frac{d\varepsilon_1}{dt} = \lambda_1 \frac{S_0}{N} + \phi_1 \lambda_1 \frac{X_2}{N} - (\sigma_1 + \mu) \varepsilon_1, \quad (\text{C.5})$$

$$\frac{d\varepsilon_2}{dt} = \lambda_2 \frac{S_0}{N} + \phi_2 \lambda_2 \frac{X_1}{N} - (\sigma_2 + \mu) \varepsilon_2, \quad (\text{C.6})$$

$$\frac{d\lambda_1}{dt} = \beta_1 \sigma_1 \varepsilon_1 - (\gamma_1 + \mu) \lambda_1, \quad (\text{C.7})$$

$$\frac{d\lambda_2}{dt} = \beta_2 \sigma_2 \varepsilon_2 - (\gamma_2 + \mu) \lambda_2. \quad (\text{C.8})$$

Now assume $\phi_1 = \phi_2 = 1$ and let $Z_i = S_0 + X_i$, $i = 1, 2$

$$\frac{dS_0}{dt} = vN - (\lambda_1 + \lambda_2) \frac{S_0}{N} - \mu S_0, \quad (\text{C.9})$$

$$\frac{dZ_1}{dt} = vN - \lambda_2 \frac{Z_1}{N} - \mu Z_1, \quad (\text{C.10})$$

$$\frac{dZ_2}{dt} = vN - \lambda_1 \frac{Z_2}{N} - \mu Z_2, \quad (\text{C.11})$$

$$\frac{dS_{12}}{dt} = \lambda_2 \frac{Z_1 - S_0}{N} + \lambda_1 \frac{Z_2 - S_0}{N} - \mu S_{12}, \quad (\text{C.12})$$

$$\frac{d\varepsilon_1}{dt} = \lambda_1 \frac{Z_2}{N} - (\sigma_1 + \mu) \varepsilon_1, \quad (\text{C.13})$$

$$\frac{d\varepsilon_2}{dt} = \lambda_2 \frac{Z_1}{N} - (\sigma_2 + \mu) \varepsilon_2, \quad (\text{C.14})$$

$$\frac{d\lambda_1}{dt} = \beta_1 \sigma_1 \varepsilon_1 - (\gamma_1 + \mu) \lambda_1, \quad (\text{C.15})$$

$$\frac{d\lambda_2}{dt} = \beta_2 \sigma_2 \varepsilon_2 - (\gamma_2 + \mu) \lambda_2. \quad (\text{C.16})$$

These equations decouple into two dynamically distinct systems $(Z_1, \lambda_2, \varepsilon_2)$ and $(Z_2, \lambda_1, \varepsilon_1)$:

$$\frac{dZ_1}{dt} = vN - \lambda_2 \frac{Z_1}{N} - \mu Z_1, \quad (\text{C.17})$$

$$\frac{d\varepsilon_2}{dt} = \lambda_2 \frac{Z_1}{N} - (\sigma_2 + \mu) \varepsilon_2, \quad (\text{C.18})$$

$$\frac{d\lambda_2}{dt} = \beta_2 \sigma_2 \varepsilon_2 - (\gamma_2 + \mu) \lambda_2, \quad (\text{C.19})$$

$$\frac{dZ_2}{dt} = vN - \lambda_1 \frac{Z_2}{N} - \mu Z_2, \quad (\text{C.20})$$

$$\frac{d\varepsilon_1}{dt} = \lambda_1 \frac{Z_2}{N} - (\sigma_1 + \mu) \varepsilon_1, \quad (\text{C.21})$$

$$\frac{d\lambda_1}{dt} = \beta_1 \sigma_1 \varepsilon_1 - (\gamma_1 + \mu) \lambda_1. \quad (\text{C.22})$$

References

- Abu-Raddad, L.J., Ferguson, N.M., 2004. The impact of cross-immunity, mutation and stochastic extinction on pathogen diversity. *Proc. R. Soc. London Ser. B—Biol. Sci.* 271, 2431–2438.
- Anderson, R.M., May, R.M., 1991. *Infectious Diseases of Humans: Dynamics and Control*. Oxford University Press, Oxford.
- Andreasen, V., Lin, J., Levin, S.A., 1997. The dynamics of co-circulating influenza strains conferring partial cross-immunity. *J. Math. Biol.* 35, 825–842.
- Behrman, R.E., Kliegman, R.M., 1998. *Nelson Essentials of Pediatrics*. Saunders, Philadelphia.

- Corbett, E.L., Steketee, R.W., ter Kuile, F.O., Latif, A.S., Kamali, A., Hayes, R.J., 2002. HIV-1/AIDS and the control of other infectious diseases in Africa. *Lancet* 359, 2177–2187.
- Corbett, E.L., Watt, C.J., Walker, N., Maher, D., Williams, B.G., Raviglione, M.C., Dye, C., 2003. The growing burden of tuberculosis: global trends and interactions with the HIV epidemic. *Arch. Intern. Med.* 163, 1009–1021.
- Cummings, D.A.T., Schwartz, I.B., Billings, L., Shaw, L.B., Burke, D.S., 2005. Dynamics effects of antibody-dependent enhancement on the fitness of viruses. *Proc. Natl Acad. Sci. USA* 102, 15259–15264.
- Cyranoski, D., 2001. Outbreak of chicken flu rattles Hong Kong. *Nature* 412, 261.
- Dobson, A.P., 2004. Population dynamics of pathogens with multiple host species. *Am. Nat.* 164, S64–S78.
- Dietz, K., 1979. Epidemiologic interference of virus populations. *J. Math. Biol.* 8, 291–300.
- Earn, D.J.D., Dushoff, J., Levin, S.A., 2002. Ecology and evolution of the flu. *Trends Ecol. Evol.* 17, 334–340.
- Elveback, L., Ackerman, E., Young, G., Fox, J.P., 1968. A stochastic model for competition between viral agents in the presence of interference. *Am. J. Epidemiol.* 87, 373–384.
- Ferguson, N.M., Anderson, R., Gupta, S., 1999. The effect of antibody-dependent enhancement on the transmission dynamics and persistence of multiple-strain pathogens. *Proc. Natl Acad. Sci. USA* 96, 790–794.
- Ferguson, N.M., Galvani, A.P., Bush, R.M., 2003. Ecological and immunological determinants of influenza evolution. *Nature* 422, 428–433.
- Gog, J., Woodroffe, R., Swinton, J., 2002. Disease in endangered metapopulations: the importance of alternative hosts. *Proc. R. Soc. London Ser. B—Biol. Sci.* 269, 671–676.
- Gumel, A.B., Moghadas, S.M., Yuan, Y., Yu, P., 2003. Bifurcation and stability analysis of a 13-d SEIC model using normal form reduction and numerical analysis. *Dynamics Continuous Discrete Impulsive Systems Ser. B. Appl. Algorithms* 10, 317–330.
- Gupta, S., Swinton, J., Anderson, R.M., 1994. Theoretical-studies of the effects of heterogeneity in the parasite population on the transmission dynamics of malaria. *Proc. Roy. Soc. London Ser. B—Biol. Sci.* 256, 231–238.
- Gupta, S., Ferguson, N., Anderson, R., 1998. Chaos, persistence, and evolution of strain structure in antigenically diverse infectious agents. *Science* 280, 912–915.
- Halstead, S.B., 1970. Observations related to pathogenesis of DHF. VI. Hypotheses and discussion. *Yale J. Biol. Med.* 42, 350–361.
- Holt, R.D., 1977. Predation, apparent competition, and structure of prey communities. *Theor. Popul. Biol.* 12, 197–229.
- Huang, Y., Rohani, P., 2005. The dynamical implications of disease interference: correlations and coexistence. *Theor. Popul. Biol.* 68, 205–215.
- Huang, Y., Rohani, P., 2006. Age-structured effects and disease interference in childhood infections. *Proc. R. Soc. London Ser. B—Biol. Sci.* 273, 1229–1237.
- Hudson, P., Greenman, J., 1998. Competition mediated by parasites: biological and theoretical progress. *Trends Ecol. Evol.* 13, 387–390.
- Kamo, M., Sasaki, A., 2002. The effect of cross-immunity and seasonal forcing in a multi-strain epidemic model. *Physica D* 165, 228–241.
- Kermack, W.O., McKendrick, A.G., 1927. A contribution to the mathematical theory of epidemics. *Proc. R. Soc. London Ser. A* 115, 700–721.
- Kirschner, D., 1999. Dynamics of co-infection with *M. tuberculosis* and HIV-1. *Theor. Popul. Biol.* 55, 94–109.
- Klingel, K., Hohenadl, C., Canu, A., Albrecht, M., Seemann, M., Mall, G., Kandolf, R., 1992. Ongoing enterovirus-induced myocarditis is associated with persistent heart muscle infection: quantitative analysis of virus replication, tissue damage, and inflammation. *Proc. Natl Acad. Sci. USA* 89, 314–318.
- Koelle, K., Rodo, X., Pascual, M., Yunus, M., Mostafa, G., 2005. Refractory periods and climate forcing in cholera dynamics. *Nature* 436, 696–700.
- Lipsitch, M., et al., 2003. Transmission dynamics and control of severe acute respiratory syndrome. *Science* 300, 1966–1970.
- Mackenzie, J.S., Gubler, D.J., Petersen, L.R., 2004. Emerging flaviviruses: the spread and resurgence of Japanese encephalitis, West Nile and dengue viruses. *Nature Med.* 10, S98–S109.
- Nowak, M.A., May, R.M., 1994. Superinfection and the evolution of parasite virulence. *Proc. Natl Acad. Sci. USA* 91, 4877–4881.
- Nowak, M.A., May, R.M., 1995. Coinfection and the evolution of parasite virulence. *Proc. R. Soc. London Ser. B—Biol. Sci.* 261, 209–215.
- Openshaw, P.J., 2005. Antiviral immune responses and lung inflammation after respiratory syncytial virus infection. *Proc. Am. Thorac. Soc.* 2, 121–125.
- Openshaw, P.J., Tregoning, J.S., 2005. Immune responses and disease enhancement during respiratory syncytial virus infection. *Clin. Microbiol. Rev.* 18, 541–555.
- Pease, C.M., 1987. An evolutionary epidemiological mechanism, with applications to type A influenza. *Theor. Popul. Biol.* 31, 422–452.
- Porco, T.C., Small, P.M., Blower, S.M., 2001. Amplification dynamics: predicting the effect of HIV on tuberculosis outbreaks. *J. Acquired Immune Deficiency Syndr.* 28, 437–444.
- Read, A.F., Taylor, L.H., 2001. The ecology of genetically diverse infections. *Science* 292, 1099–1102.
- Rohani, P., Earn, D.J.D., Finkenstadt, B.F., Grenfell, B.T., 1998. Population dynamic interference among childhood diseases. *Proc. R. Soc. London Ser. B—Biol. Sci.* 265, 2033–2041.
- Rohani, P., Green, C.J., Mantilla-Beniers, N.B., Grenfell, B.T., 2003. Ecological interference among fatal infections. *Nature* 422, 885–888.
- Rohani, P., Wearing, H.J., Vasco, D.A., Huang, Y., 2006. Understanding host-multi-pathogen systems: the interaction between ecology and immunology. In: Osfeld, R., Keesing, F., Eviner, V. (Eds.), *Ecology of Infectious Diseases*. Princeton University Press, Princeton.
- Thompson, W.W., Shay, D., Weintraub, E., Brammer, L., Cox, N., Anderson, L., Fukuda, K., 2003. Mortality associated with influenza and respiratory syncytial virus in the united states. *J. Am. Med. Assoc.* 289, 179–186.
- Tomkins, D.M., Greenman, J.V., Hudson, P.J., 2001. Differential impact of a shared nematode parasite on two gamebird hosts: implications for apparent competition. *Parasitology* 122, 187–193.
- Wearing, H.J., Rohani, P., 2006. Ecological and immunological determinants of dengue epidemics. *Proc. Natl Acad. Sci.* 103, 11802–11807.
- White, L.J., Cox, M.J., Medley, G.F., 1998. Cross immunity and vaccination against multiple microparasite strains. *IMA J. Math. Appl. Med. Biol.* 15, 211–233.